Oecologia (2021) 196:863–875
https://doi.org/10.1007/s00442-021-04966-z

ECOSYSTEM ECOLOGY – ORIGINAL RESEARCH

Ectomycorrhizal fungi are associated with reduced nitrogen cycling rates in temperate forest soils without corresponding trends in bacterial functional groups

Mustafa Saifuddin[1] · Jennifer M. Bhatnagar[1] · Richard P. Phillips[2] · Adrien C. Finzi[1]

Received: 10 September 2020 / Accepted: 9 June 2021 / Published online: 25 June 2021

Abstract

Microbial processes play a central role in controlling the availability of N in temperate forests. While bacteria, archaea, and fungi account for major inputs, transformations, and exports of N in soil, relationships between microbial community structure and N cycle fluxes have been difficult to detect and characterize. Several studies have reported differences in N cycling based on mycorrhizal type in temperate forests, but associated differences in N cycling genes underlying these fluxes are not well-understood. We explored how rates of soil N cycle fluxes vary across gradients of mycorrhizal abundance (hereafter "mycorrhizal gradients") at four temperate forest sites in Massachusetts and Indiana, USA. We paired measurements of N-fixation, net nitrification, and denitrification rates with gene abundance data for specific bacterial functional groups associated with each process. We find that the availability of NO_3 and rates of N-fixation, net nitrification, and denitrification are reduced in stands dominated by trees associated with ECM fungi. On average, rates of N-fixation and denitrification in stands dominated by trees associated with arbuscular mycorrhizal fungi were more than double the corresponding rates in stands dominated by trees associated with ectomycorrhizal fungi. Despite the structuring of flux rates across the mycorrhizal gradients, we did not find concomitant shifts in the abundances of N-cycling bacterial genes, and gene abundances were not correlated with process rates. Given that AM-associating trees are replacing ECM-associating trees throughout much of the eastern US, our results suggest that shifts in mycorrhizal dominance may accelerate N cycling independent of changes in the relative abundance of N cycling bacteria, with consequences for forest productivity and N retention.

Keywords Nitrogen cycling · Mycorrhizal fungi · Soil biogeochemistry

Introduction

Nitrogen (N) availability can be a primary constraint on productivity in temperate forests (LeBauer and Treseder 2008; Vitousek and Howarth 1991; Xia and Wan 2008), yet quantifying N cycling rates remains a significant challenge. Long-term datasets are regularly unable to identify processes responsible for sizable accumulations and losses of N in temperate forests, and much of this is attributed to uncertainties in soil microbial transformations of N, including N-fixation, nitrification, and denitrification (Bormann 1993; Bormann et al. 2002; Yanai et al 2012, 2013). Each of these N cycle fluxes is carried out by distinct microbial functional groups, and characterizing controls on the abundances and activities of these microbial groups is critical to an improved understanding of N cycling (Berthrong et al. 2014; Enanga et al. 2017; Hsu and Buckley 2009; Lennon and Houlton 2017; Wallenstein and Vilgalys 2005). In soil, heterotrophic bacteria are subject to complex interactions with plant roots, mycorrhizal fungi, and other soil organisms, which all have the potential to impact the activity and abundance of N cycling functional groups and subsequently impose variation in N cycling across stand types (e.g., Ribbons et al. 2018; Mushinski et al. 2019; Qin et al. 2019; Kelly et al. 2021).

In temperate forests, nearly all trees associate with either arbuscular mycorrhizal (AM) or ectomycorrhizal (ECM) fungi, and differences between these two groups of mycorrhizal fungi have key implications for biogeochemical

Communicated by Hakan Wallander.

✉ Adrien C. Finzi
afinzi@bu.edu

[1] Boston University, Boston, USA

[2] Indiana University, Bloomington, USA

cycling (Averill et al. 2014; Craig et al. 2018a, b; Phillips et al. 2013). Nitrogen cycling, in particular, is considered to be more "open" in AM-dominated stands relative to ECM-dominated stands (Finzi et al. 1998; Phillips et al. 2013; Lin et al. 2017). Such differences may arise from mycorrhizal group differences in litter quality (Cornelissen et al. 2001; Keller and Phillips 2019a, b; Averill et al. 2019), litter-induced changes in soil acid–base chemistry (Finzi et al. 1998; Mushinski et al. 2019; Lin et al. in revision), root or mycorrhizal partitioning of N forms (Chen et al. 2016; Goodale 2016; Liese et al. 2018), or root or mycorrhizal-induced changes in decomposition (Averill and Hawkes, 2016). While no single factor is likely to be responsible for observed N cycling differences, all of the aforementioned processes involve N transformations or competitive interactions mediated by groups of soil microorganisms.

ECM fungi are able to produce a wide range of enzymes including those targeting plant substrates such as cutin, lipids, waxes, pectin, cellulose, cellobiose, hemicellulose, polyphenols, and lignin (Read and Perez-Moreno 2003). In contrast, AM fungi have a much narrower profile of enzyme capacities, typically a reduced complement of enzymes that break down organic matter and are primarily associated with the uptake of inorganic N (Read and Perez-Moreno 2003). Due to their broader enzyme capacities, ECM fungi are able to compete directly with free-living saprotrophs for access to organic substrates (Cornelissen et al. 2001; Gadgil and Gadgil 1975; Phillips et al. 2013; Sterkenburg et al. 2018), which can reduce rates of heterotrophic respiration (Averill and Hawkes, 2016) and decomposition (Averill et al. 2014, 2018). This competition can slow N mineralization, leading to elevated ratios of organic N to inorganic N pools in ECM-associated stands relative to AM-associated stands (Finzi and Berthrong 2005; Phillips et al. 2013). Likewise, accelerated litter decay by saprotrophs in AM-dominated stands can lead to accelerated rates of N mineralization and nitrification (Finzi et al. 1998; Lovett et al. 2004; Midgley and Phillips 2016), which may allow AM-associated trees to acquire N primarily in inorganic forms (Gallet-Budynek et al. 2009; Lovett et al. 2004; Midgley and Phillips 2014). Despite the critical importance of N cycling saprotroph activity in these patterns, differences in the community structure of N cycling saprotrophic bacteria between AM- and ECM-dominated stands have not been widely characterized (but see Mushinski et al. 2020). Furthermore, to our knowledge, no studies to date have characterized rates of N-fixation and denitrification in tandem across mycorrhizal gradients.

Identifying relationships between microbial community structure and biogeochemical function has been a major goal in microbial biogeochemistry, especially in the context of understanding how shifts in community structure might impact ecosystem processes (Allison and Martiny 2008; McGuire and Treseder 2010). Measures of gene abundances are often used to describe the functional potential of microbial communities and broadly characterize their structure as related to biogeochemical cycling (e.g., Wallenstein and Vilgalys 2005; Hsu and Buckley 2009; Berthrong et al. 2014; Levy-Booth et al. 2014; Bier et al. 2015; Rocca et al. 2015; Kelly et al. 2021). However, characterizing these relationships has proven difficult due to the high diversity of soil microbial communities, potential functional redundancy across taxa, dormancy, and abiotic controls on activity (Bier et al. 2015). Relatively few studies in temperate forest ecosystems pair targeted measurements of gene abundances with their associated biogeochemical flux or pools measurements (Rocca et al. 2015), despite the presence of clearly-delineated bacterial functional groups in the N cycle. Among studies which do pair process rate measurements with gene abundances, the strongest relationships are often shown for specific pathways in the N cycle, such as nitrification (Bier et al. 2015).

Understanding how the genetic capacity of and emergent activities of microbial communities vary in relation to mycorrhizal type may help clarify the underlying mechanisms responsible for variation in N cycling patterns between AM- and ECM-associated forest stands. The genetic basis for N-fixation, nitrification, and denitrification has been well-characterized (Levy-Booth et al. 2014), providing a unique system in which gene abundances can be linked with biogeochemical flux measurements (Hsu and Buckley 2009; Reed et al. 2010; Wallenstein and Vilgalys 2005; Mushinski et al. 2020). In this study, we paired measurements of microbial N cycling with abundance measurements for specific bacterial N-cycling genes along gradients of mycorrhizal type. We collected samples from replicate mycorrhizal gradients at temperate forest sites in Indiana and Massachusetts, USA with variable tree composition and site characteristics. First, we explored how rates of N-fixation, net nitrification, and denitrification are structured in relation to proportions of AM- and ECM-associated tree species at the plot-level. We hypothesized that the commonly observed faster N cycling rates in AM stands would result in these stands having greater N fixation rates but also faster denitrification rates. Second, we explored whether these differences in flux rates were associated with differences in microbial community structure. We hypothesized that rates of a particular N cycling pathway are positively correlated with the abundance of genes involved in the pathway.

Materials and methods

Site descriptions

This research was conducted at 48 plots (15 m x 15 m) along four mycorrhizal gradients established in temperate hardwood forests. Two gradients, each consisting of nine

plots (15 m x 15 m), were located in southern Indiana, USA at the Griffy Woods (GW, 39°11′N, 86°30′W) and Lilly-Dickey Woods (LD, 39°14′N, 86°13′W). These plots are described in further detail in Cheeke et al. 2017 and Johnson et al. 2018. Soils at Griffy Woods are loamy-skeletal, mixed, active, mesic Typic Dystrudepts and Hapludults in the Brownstown–Gilwood complex. Soils at Lilly-Dickey Woods are loamy-skeletal, mixed, active, mesic Typic Dystrudepts, Ultic Hapludalfs, and Typic Hapludults in the Berks-Trevlac-Wellston complex. The trees at GW are ~ 90 years old and the forest has little understory due to high deer densities (Shelton et al. 2014). Lilly-Dickey Woods has trees exceeding 150 years and the understory is characterized by lots of structure (due to low deer densities) and abundant coarse woody debris (Johnson et al. 2018). Soils in these forests are unglaciated, silty-loams derived from sandstone, shale, and limestone (Craig et al. 2018a, b). Mean annual precipitation is 120 cm and mean annual temperature is 11.6 °C (Cheeke et al. 2017; Phillips et al. 2013).

Two gradients, each consisting of 15 plots (15 m x 15 m), were located at the Prospect Hill (PH) and Simes (SM) tracts of the Harvard Forest Long Term Ecological Research Site (42.58 N, 72.188 W) in Petersham, Massachusetts, USA. Soils at these sites are inceptisols classified as Typic Dystrochrepts derived from glacial till overlying granite–schist–gneiss bedrock (USDA Natural Resources Conservation Service, Web Soil Survey). Mean annual precipitation is 110 cm and mean annual temperature is 8 °C.

At each plot, all trees over 5 cm diameter at breast height were measured, identified to species-level, and classified by mycorrhizal type to determine the proportion of tree basal area associated with AM and ECM fungi (Phillips et al. 2013). The proportion of AM-associated trees at the plot-level ranges from all AM-associated to all ECM-associated. At plots located in Harvard Forest, dominant tree species include *Quercus rubra* (ECM), *Acer rubrum* (AM), *Acer saccharum* (AM), *Fraxinus americana* (AM), and *Betula lenta* (ECM). At plots located in southern Indiana, dominant tree species include *Acer saccharum* (AM), *Quercus rubra* (ECM), *Quercus alba* (ECM), *Liriodendron tulipifera* (AM), and *Fraxinus americana* (AM).

Soil sampling and soil properties

Four 0–15 cm mineral horizon soil cores were collected from each plot and transported on ice to Boston University, MA, USA. Replicate cores were composited at the plot level. Due to variation in the depth of the organic horizon across the gradients, we chose to focus our analysis on the mineral horizon to allow for comparisons across all plots. Soils were sieved to < 2 mm in the lab following collection to remove large roots and rocks. Gravimetric soil moisture was measured based on mass loss following evaporation. Soil pH was measured with a pH probe placed in soil pastes prepared at a 1:10 ratio of soil to deionized water. Total soil C and N content were measured via flash combustion on a Thermoquest NC 2500 elemental autoanalyzer.

Inorganic N pools and nitrification rates

Total inorganic N extractions were completed using 20 g field-moist soil and 100 mL 2 M KCl. Concentrations of NO_3 and NH_4 in extractant were quantified using colorimetric microplate assays followed by spectrophotometry with a Versamax microplate reader (Molecular Devices; Sims et al. 1995; Doane and Horwáth 2003). Samples were incubated at room temperature for up to 28 days. Because these measurements were made at constant lab temperature (~ 22.5 °C), we considered them to reflect potential – rather than absolute – rates of net N mineralization or nitrification. Potential net nitrification (μg N g soil − 1 d − 1) was calculated as the difference in NO_3^- measured between the two timepoints for a given sample, divided by the incubation period. Potential net N mineralization (μg N g $soil^{-1}$ d^{-1}) was calculated as the difference in total inorganic N (NO_3-N + NH_4-N) between the two timepoints for a given sample, divided by the incubation period.

Potential N-fixation

Three 5 g subsamples of bulk soil from each plot ($n = 48$) were incubated in gas-tight vials with a mixture of 80% N_2 and 20% O_2 gas for nine days following the date of sampling. Controls received natural abundance N_2, while treatments received 98 atom% enriched $^{15}N_2$ gas with a glucose slurry to measure potential rates in the absence of C-limitation (Hsu & Buckley, 2009). Following the incubation period, samples were dried, ground, and analyzed using an isotope ratio mass spectrometer at the Boston University Stable Isotope Laboratory. Net potential N-fixation was calculated based on the difference in total ^{15} N in treatments compared to control samples based on an isotopic mixing model as described in Montoya et al. (1996).

Denitrification

For samples from a subset of sites across the gradients ($n = 30$), 20 g of soil were placed in a mason jar and incubated with 2 mL of a solution containing 16 μg of 98 atom% enriched $K^{15}NO_3$-N. Gas samples of 10 mL were collected through rubber septa attached to the mason jars immediately following labeling and after 24 h. Gas samples were transferred to evacuated exetainers and concentrations of $^{15}N_2O$ gas were analyzed at the UC Davis Stable Isotope Facility using a ThermoScientific GasBench and Precon gas concentration system paired with a ThermoScientific Delta V

Plus isotope-ratio mass spectrometer (Bremen, Germany). Denitrification rates were calculated based on the difference in $^{15}N_2O$ in samples collected after 24 h of incubation with $K^{15}NO_3$ and initial concentrations of $^{15}N_2O$ at start of incubation, as described in Arah (1992).

Molecular analyses

For all samples from the Harvard Forest, rhizosphere soil was manually separated from bulk soil on the date of sampling by gently agitating plant roots by hand and isolating clusters of soil remaining adhered to roots using forceps (Finzi et al. 2015; Phillips and Fahey 2006). This separation was not performed for samples from Indiana due to a longer transportation time on ice (< 24 h). Instead, all samples were sieved < 2 mm and the four composite cores from each plot were combined and mixed to homogenize. DNA was extracted in triplicate for 0.25 g subsamples of soils using MoBio PowerSoil DNA kits. Following extraction and quality-checking using a NanoDrop spectrophotometer, replicate DNA extractions per soil subsample were pooled. Quantitative PCR (qPCR) was performed using primer sets and annealing temperatures published in Levy-Booth et al. (2014) to quantify the abundances of *nifH*, *amoA* and *nosZ*. The gene *nifH* codes for the enzyme nitrogenase, which catalyzes N-fixation. The gene *amoA* codes for the alpha-subunit of the ammonium oxidase enzyme, which is involved in nitrification. The gene *nosZ* codes for the catalytic subunit of nitrous oxide reductase, which is involved in denitrification. While other genes are involved in additional steps along each of these pathways, this subset of genes allowed us to characterize one gene per pathway. Standard curves (Wallenstein and Vilgalys 2005) were calculated based on a serial dilution of gBlocks (linear DNA fragments) containing amplicon regions for each respective gene synthesized by Integrated DNA Technologies (Coralville, IA). All reactions were performed in triplicate in 384-well microplates using ABsolute qPCR Master Mix, containing SYBR Green and ROX, on an ABI 7900ht qPCR machine.

Statistical analyses

All statistical analyses were conducted using Rstudio v. 1.1.383 (R Core Team 2017). To explore how N cycling rates and gene abundances vary in relation to mycorrhizal abundance, generalized linear models (GLMs) with gamma-distributions and inverse link functions were analyzed using the proportion of ECM-associated basal area at the plot level and site as predictor variables and rates of N-fixation, net nitrification, denitrification, or gene abundances of *nifH*, *amoA*, or *nosZ* as response variables. To explore relationships between gene abundances and N pool sizes, we analyzed GLMs with gene abundances as response variables and inorganic N pool concentrations associated with each respective gene as predictors. Similarly, we used a series of GLMs to explore gene-flux relationships with *nifH* regressed against N-fixation rates, *amoA* regressed against net nitrification rates, and *nosZ* regressed against denitrification rates. With 48 samples, the lowest correlation detectable with a power of 80% is 0.39.

We used stepwise Akaike's information criterion (AIC) model selection to explore more complex models of N-fixation, nitrification and denitrification rates. The *stepAIC* function in the *MASS* package (Venables & Ripley, 2002) with "both" set as the mode of stepwise search was used to compare models with proportion ECM basal area, total basal area, *Acer saccharum* basal area, soil pH, and inorganic N concentrations as potential predictors of N-fixation and net nitrification rates. Similarly, we used a model with proportion ECM basal area, total basal area, *Acer saccharum* basal area and soil pH as potential predictors of denitrification rates. We chose to include *Acer saccharum* basal area in these models due to interest in the potential for this tree species to drive N cycling patterns (Finzi et al. 1998; Phillips et al. 2013; Templer et al. 2005). We computed the second-order AIC (AICc) to correct for small sample sizes using the *performance_aicc* function in the *performance* package (Lüdecke et al. 2020). This analysis allowed us to compare the full model with all parameters above with the simplest model suggested through the stepwise search.

Additionally, we classified plots as AM-dominated (> 70% AM), ECM-dominated (> 70% ECM), or mixed (30–70% ECM), and used these classifications as categorical variables ($n = 16$ for AM plots, $n = 20$ for ECM plots, and $n = 12$ for mixed) in the analysis of variance (ANOVA) tests. We used the Tukey test of honest significant differences to compare flux rates, N pools and gene abundances across these classifications. Gene abundances and rates of net nitrification were log-transformed in these analyses. Rates of denitrification were averaged across 2016 and 2017 at the stand-level for samples from Harvard Forest.

Results

N availability

The concentration of extractable NO_3 ranged from 0 to 6.15 µg NO_3-N/g soil across all plots, with a mean of 0.96 ± 0.2 µg NO_3-N/g soil (SE). Nitrate pool sizes consistently declined with increasing ECM-associated basal area ($p < 0.01$, Table 2, Fig. 1A), with mean nitrate pool sizes in stands dominated exclusively by ECM-associated trees (0.24 ± 0.07 µg NO_3-N/g soil) significantly reduced compared to mean nitrate availability in stands dominated by

AM-associated trees (2.13 ± 0.46 µg NO_3-N/g soil, Figure S1A, Table 1).

In contrast, ammonium pool sizes were not correlated with ECM-associated basal area (p = 0.72, Table 2, Fig. 1a) and was not significantly different between AM-dominated and ECM-dominated stands ($p = 0.99$, Table 1). Ammonium availability ranged from 0 to 7.33 µg NO_3-N/g soil with a mean of 2.84 ± 0.33 µg NH_4-N/g soil (Figure S1A).

On average, NH_4 availability exceeded NO_3 availability. However, we observed differing patterns between tracts, with plots located in Indiana showing lower mean NO_3-N availability (0.55 ± 0.34) and higher mean NH_4-N availability (4.87 ± 0.40) compared to plots in Massachusetts (1.21 ± 0.23 µg NO_3-N/g soil and 1.6 ± 0.30 µg NH_4-N/g soil). The ratio of NO_3 to NH_4 at the plot level tended to be higher at the Massachusetts sites (1.4 ± 2.5) compared to at the Indiana sites (0.46 ± 1.2).

Soil N ranged from 0.26 to 1.23% by mass, with a mean of 0.26 ± 0.03%. The sites located in Massachusetts had higher mass percent N values on average (0.33 + 0.04) than the sites located in Indiana (0.13 ± 0.01). Across all sites, soil N declined with increasing ECM-associated basal area ($p < 0.001$, Fig. 1c, Table 2). Similarly, the ratio of soil C:N increased with increasing ECM-associated basal area ($p < 0.001$, Table 2, Fig. 1d), indicating reductions in the availability of N relative to C. This relationship was significant across plots at both sites (Indiana and Massachusetts), but was stronger for plots located in Massachusetts ($p < 0.001$; $R^2 = 0.55$) than for plots located in Indiana ($p < 0.05$; $R^2 = 0.22$).

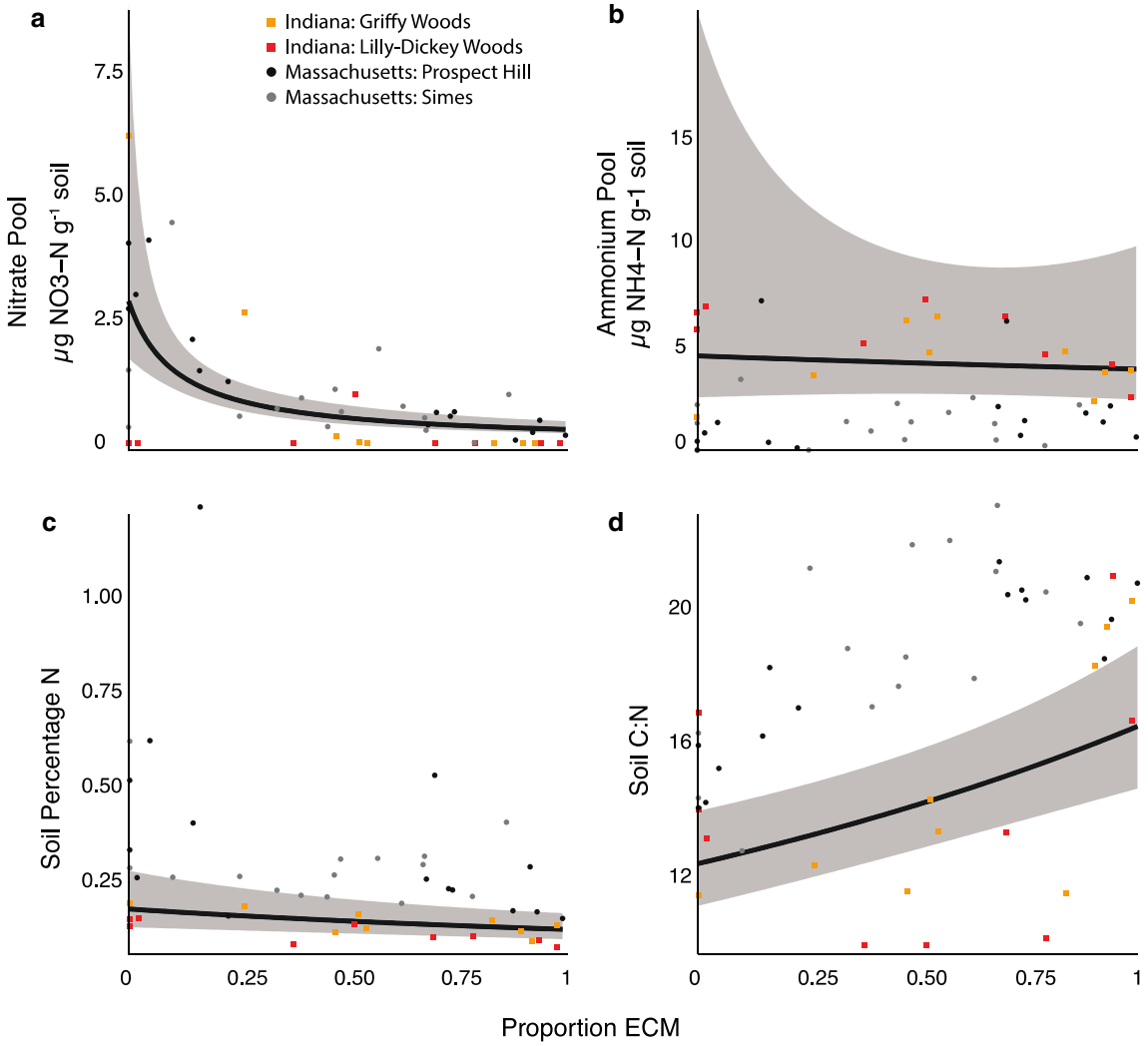

Fig. 1 Soil N pools across gradients. **a** NO_3 (µg NO_3-N/g soil), **b** NH_4 (µg NH_4-N/g soil), **c** soil percent N, and **d** soil C:N versus proportion of plot area associated with ECM

Table 1 N pools and fluxes summary

	ECM		Mixed		AM	
	Median	IQR	Median	IQR	Median	IQR
NO_3*** (μg NO_3-N g^{-1} soil)	0.24	0.51	0.70	0.61	2.08	2.60
NH_4 (μg NH4-N g^{-1} soil)	1.96	1.74	1.83	0.61	1.31	3.06
NO_3:NH_4**	0.17	0.38	0.46	0.84	3.03	5.77
Soil percentage N*	0.22	0.14	0.22	0.09	0.29	0.29
Soil C:N**	20.31	1.38	17.84	3.08	15.19	2.50
Potential N-fixation* (μg N kg^{-1} soil day^{-1})	17.85	29.05	14.5	33.8	34.60	43.60
Net nitrification*** (μg NO_3-N g^{-1} soil day^{-1})	0.05	0.07	0.13	0.20	0.30	0.49
Potential denitrification* (μg N_2O-N kg^{-1} soil day^{-1})	0.17	0.50	0.02	15.30	12.1	15.84

IQR = difference between 75 and 25% quartiles. ECM = ≥ 70% Ectomycorrhizal-associated basal area, MIX = 31–69% Ectomycorrhizal-associated basal area, AM = ≤ 30% ECM- Ectomycorrhizal-associated basal area

***$p < 0.001$, **$p < 0.01$, *$p < 0.05$ from Tukey's test. Significance values are for comparison between AM and ECM stands.

Table 2 GLM regression summaries for N pools or flux in row as response and plot proportion ECM and site as predictors

	Standard error	*T* value	*P* value	Cox-Snell Pseudo R^2
NO_3** (μg NO_3-N g^{-1} soil)	0.31	0.67	< 0.01	0.14
NH_4 (μg NH_4-N g^{-1} soil)	0.10	0.36	0.72	0.14
NO_3:NH_4	1.10	1.95	0.06	0.11
Soil percentage N***	0.64	3.55	< 0.001	0.68
Soil C:N***	0.004	-4.84	< 0.001	0.56
Potential N-fixation*(μg N kg^{-1} soil day^{-1})	0.01	2.46	< 0.05	0.04
Net nitrification*** (μg NO_3-N g^{-1} soil day^{-1})	3.57	3.94	< 0.001	0.18
Potential denitrification (μg N_2O-N kg^{-1} soil day^{-1})	0.15	1.12	0.28	0.60

Nitrogen cycling rates

Rates of potential N-fixation, net nitrification and denitrification all showed negative relationships with increasing ECM tree dominance. Potential N-fixation rates ranged from 0 to 139.9 μg N/kg soil/day, with a mean of 32.4 ± 4.7 μg N/kg soil/day. On average, rates of fixation were higher in the plots located in Indiana (41.1 ± 6.9) than the plots located in Massachusetts (27.2 ± 6.3). Across all sites, we observed consistent declines of potential N-fixation rates with increasing ECM-associated basal area ($P < 0.05$, Fig. 2a, Table 2). Potential N-fixation rates in ECM-dominated stands were approximately 45% those of rates in AM-dominated stands on average, with mean potential N-fixation rates of 21.9 ± 5.8 μg N/kg soil/day in ECM-dominated stands compared to mean potential N-fixation rates of 10.24 ± 0.456 μg N/kg soil/day in AM-dominated stands (Table 1, Figure S2A). Ammonium availability was a significant predictor of potential N fixation rates, with greater availability of NH_4 in plots with high rates of potential N fixation.

Net nitrification rates ranged from 0 to 0.97 μg NO_3-N/g soil/day, with a mean rate of 0.18 ± 0.034 μg NO_3-N/g soil/day. On average, rates of net nitrification were similar in Massachusetts (0.18 ± 0.05) and Indiana (0.16 ± 0.05). Net nitrification rates declined with increasing ECM-associated basal area ($p < 0.001$, Fig. 2b, Table 2), and mean net nitrification rates were several times greater in AM-dominated stands (0.34 ± 0.077 μg NO_3-N/g soil/day) compared to ECM-dominated stands (0.04 ± 0.008 μg NO_3-N/g soil/day, Figure S2B, Table 1). Nitrate availability was significantly correlated with net nitrification rates ($R^2 = 0.36$, $p < 0.001$).

Denitrification rates ranged from 0 to 22.1 μg N/kg soil/day, with a mean rate of 5.92 ± 1.45 μg N_2O-N kg $soil^{-1}$ day^{-1}. On average, rates of denitrification were higher in plots located in Indiana (6.7 ± 2.0) than in plots located in Massachusetts (4.8 ± 2.1). Denitrification rates were significantly reduced in ECM-dominated stands (1.70 ± 0.92 μg N/kg soil/day) compared to AM-dominated stands (9.82 ± 2.0 μg N/kg soil/day, Figure S2C, Table 1), but were not linearly related to ECM-associated basal area ($p = 0.28$; Fig. 2c, Table 2) and. Ammonium availability was a significant predictor of denitrification rates, with greater

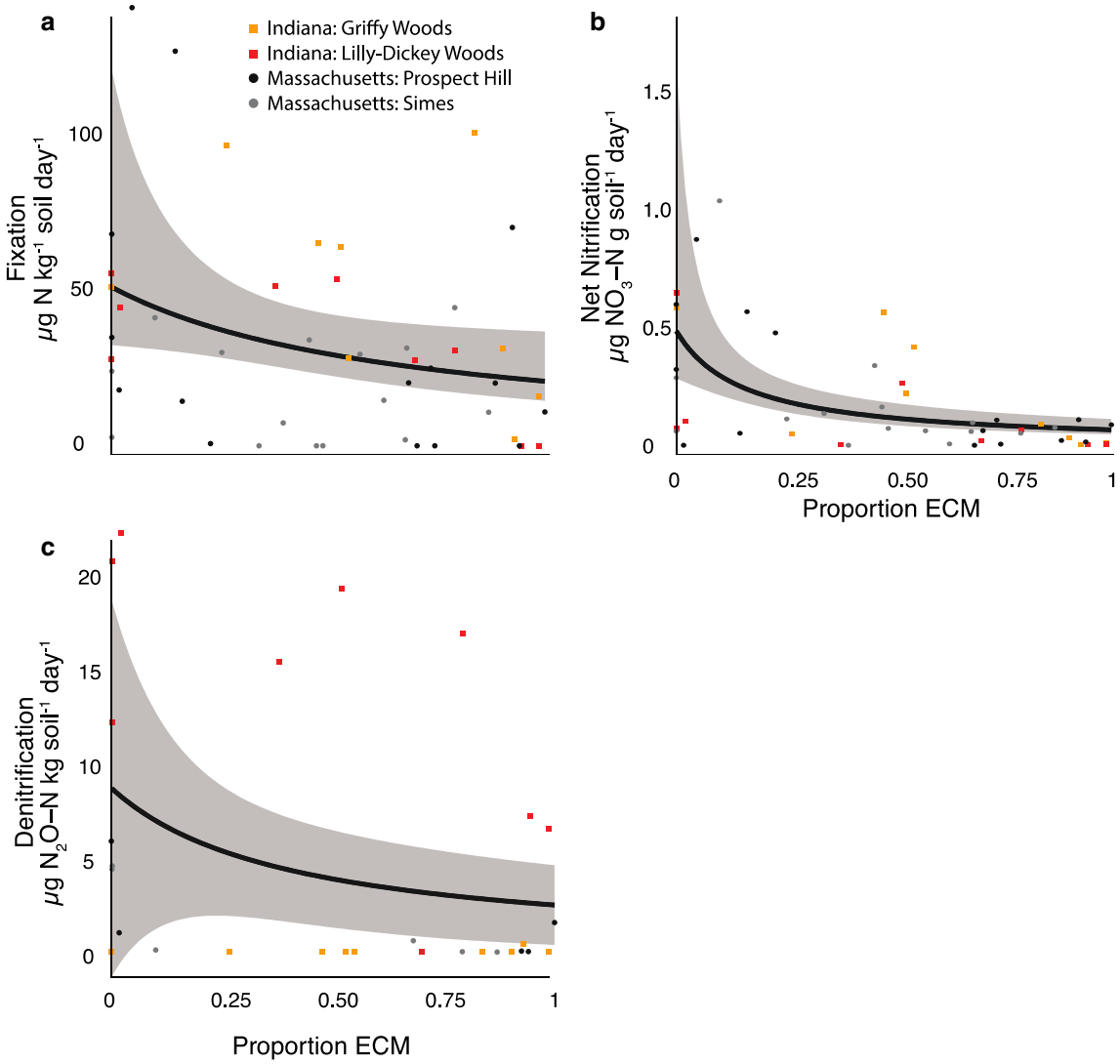

Fig. 2 Regressions of N cycle fluxes against proportion ECM. Flux rates versus proportion ECM-associated basal area. **a** Fixation (μg N/kg soil/day), **b** Net Nitrification (μg NO_3-N/g soil/day), **c** Denitrification (μg N_2O-N/kg soil/day)

availability of NH_4 in plots with high rates of denitrification ($R^2 = 0.26$, $P < 0.001$).

For all three N cycle fluxes measured, proportion of ECM basal area was supported as a predictor of flux rates outside of the effects of *Acer saccharum* basal area, total basal area or soil pH. We chose to include *Acer saccharum* basal area in these models due to interest in the potential for this tree species to drive N cycling patterns (Finzi et al. 1998; Phillips et al. 2013; Templer et al. 2005). Stepwise AIC model selection did not support inclusion of total basal area, *Acer saccharum* basal area, or pH as predictors of N-fixation. The model including the proportion of ECM basal area and NH_4 and NO_3 concentrations were supported (AICc = 158.4) over the model including all predictors (AICc = 166.4). Stepwise AIC model selection did not support inclusion of total basal area, *Acer saccharum* basal area, pH, or inorganic N concentrations as predictors of net nitrification. The model with ECM basal area as the sole predictor (AICc = -151.4) was favored over the full model (AICc = -139.8). Stepwise AIC model selection did not support inclusion of total basal area, *Acer saccharum* basal area, or pH as predictors of denitrification. The model with ECM basal area as the sole predictor (AICc = 92.6) was favored over the full model (AICc = 104.3).

Gene abundances

Overall, we found little difference in the abundances of the N cycling genes we quantified across the mycorrhizal gradients. Gene abundances for *nifH* were not related to ECM-associated basal area (Fig. 3a), rates of potential N-fixation or NH_4 pool sizes. Gene abundances for *amoA*

were not differentially associated with ECM-associated basal area (Fig. 3b), rates of nitrification, or pool sizes of NO_3 and NH_4. Gene abundances for *nosZ* were not differentially associated with ECM-associated basal area (Fig. 3c) or with rates of denitrification. Soil fraction (bulk versus rhizosphere) was a significant predictor of gene abundance for *nosZ* only.

Discussion

Identifying the role of microbial functional groups in driving differences in N cycling patterns between AM and ECM-associated stands will require an improved understanding of relationships between soil nutrient availability, microbial community structure, and N cycling rates. In this study, we paired measurements of rates of potential N-fixation, net nitrification, and denitrification rates with measurements of the abundances of corresponding bacterial N-cycling

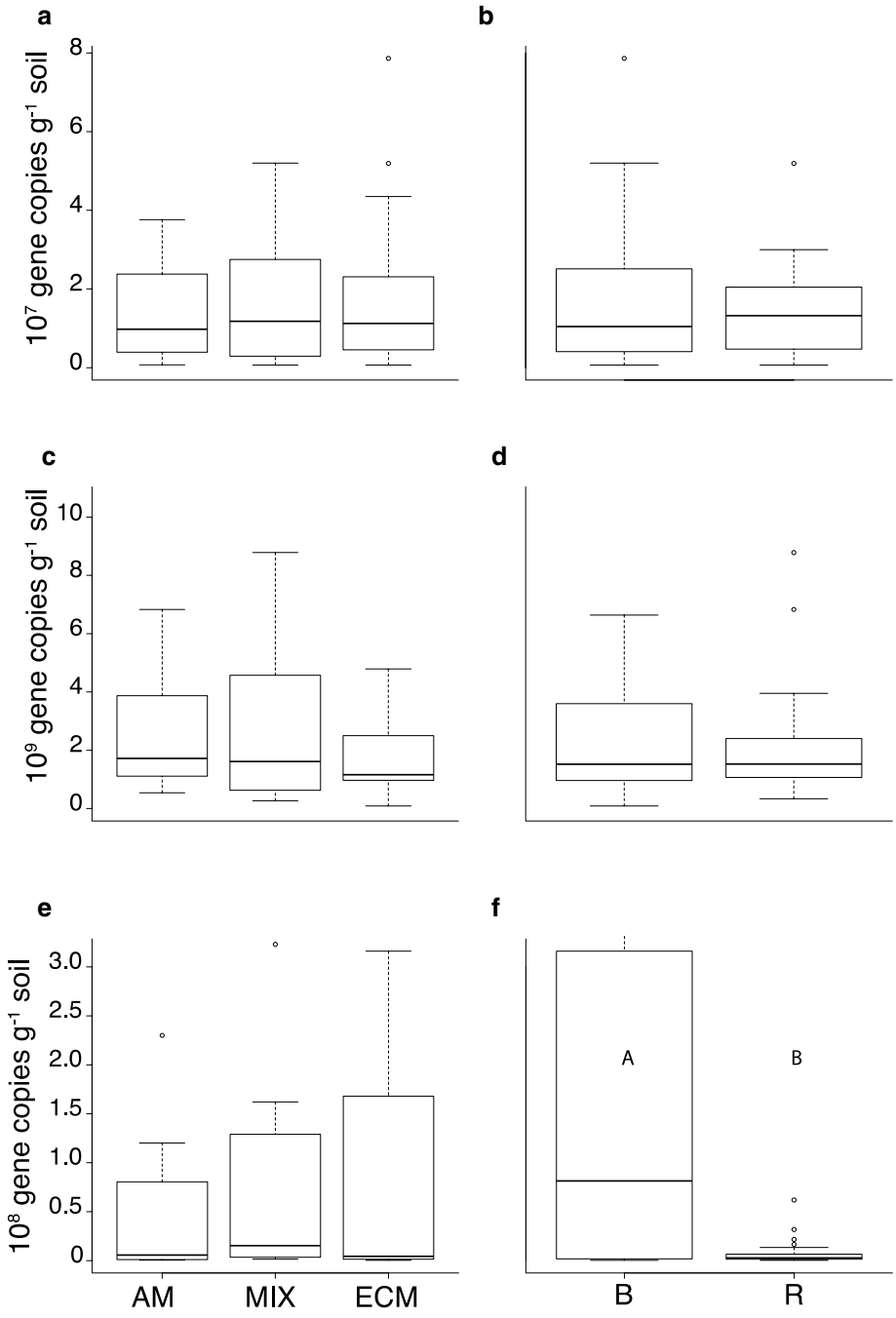

Fig. 3 Boxplots of gene abundances by plot proportion of basal area: AM (≤ 30% ECM-associated), MIX, (30–70% ECM), ECM (≥ 70% ECM-associated), and soil fraction (B = Bulk, R = Rhizosphere). **a** nifH (gene copies g^{-1} soil) by plot type and **b** by soil fraction, **c** amoA (gene copies g^{-1} soil) by plot type and **d** by soil fraction, **e** nosZ (gene copies g^{-1} soil) by plot type and **f** by soil fraction

genes across gradients of mycorrhizal abundance. To our knowledge, the present study represents the only study in which rates of N-fixation and denitrification and associated gene abundances were characterized in relation to mycorrhizal gradients. These data allowed us to first test whether mycorrhizal abundance was associated with differences in N cycling bacterial activity and nutrient availability. Consistent with our initial hypothesis, we observed decreased rates of net nitrification and inorganic N availability across multiple temperate forest sites as the abundance of ECM-associated trees increased. We additionally observed reduced rates of N-fixation and denitrification in stands dominated by ECM-associated trees. Second, we tested for relationships between selected gene abundances and corresponding flux rates across the mycorrhizal gradients. We did not find evidence to suggest that N-cycling genes varied along AM-ECM gradients, or that gene abundance was related to any metric of community-level N cycling rates, indicating a potential decoupling of N fluxes from functional group gene abundances for the limited subset of genes we analyzed.

Rates of potential N-fixation, net nitrification and denitrification were each reduced in stands dominated by ECM tree abundance across the gradients, indicating that mycorrhizal abundance significantly affects the rate of N cycling. N-fixation represents the only biotic pathway by which new N enters ecosystems from the atmosphere, making it essential to characterize in N-limited ecosystems (Reed et al. 2011). The stands we explored in this study lack tree species or shrubs that form symbiotic associations with N-fixers, making free-living diazotrophs in soil the main source of new N inputs from the atmosphere, outside of N deposition of previously-fixed N. Free-living N-fixation rates can be highly variable, responsive to multiple environmental and community controls and a substantial source of new N from the atmosphere to many terrestrial ecosystems (Reed et al. 2011). However, relatively little is known about the role of mycorrhizal type on free-living fixation. We observed N-fixation rates in AM-dominated stands nearly twice those in ECM-dominated stands, suggesting that ECM abundance may slow ecosystem N cycling over time. One mechanism for this may be a reduction in diazotrophic activity consistent with reductions in overall bacterial activity, as shown previously in the suppression of heterotrophic respiration and decomposition in the presence of ECM-fungi (Averill et al. 2014, 2018; Averill and Hawkes, 2016) and as shown recently for overall N-cycle gene and transcript copy numbers in ECM-associated stands (Mushinski et al 2020). Alternatively, labile C substrates released by AM colonized roots (Wurzburger and Brookshire 2017; Keller and Phillips 2019a, b) may provide an energy source capable of stimulating diazotrophic activity, contributing to increased N stocks in AM-dominated stands despite increased losses through nitrification and denitrification (Lovett et al. 2000; Craig et al. 2018a, b; Jo et al. 2019). Greater stimulation of rhizosphere N cycling in AM stands might arise from increases in root-derived carbon, which can be twice as large in AM-associated stands compared to ECM-associated stands (Keller et al. 2021). While rates of N-fixation are relatively small compared to other N-cycle fluxes, they play an important role over the long-term by allowing N to accumulate (Reed et al. 2011). N-fixation is an energetically costly strategy, and free-living diazotrophs may switch between particular N acquisition pathways depending on favorability (Norman and Friesen 2017). Complementing these findings of potential N-fixation with in-situ measurements of N-fixation across mycorrhizal gradients will be necessary to determine actual rates.

Nitrification represents a pathway for potential loss of inorganic N from the soil as NO_3^- in runoff or through subsequent release in gaseous forms via denitrification. This flux requires the activities of ammonia-oxidizers and nitrite-oxidizers, which are comprised of both bacteria and archaea (Levy-Booth et al. 2014). Consistent with other studies, we found the highest rates of net nitrification in AM-associated stands, while ECM-associated stands tended to show near-zero rates of net nitrification (Finzi et al. 1998; Lovett et al. 2004; Phillips et al. 2013; Lin et al. 2017; Mushinski et al. 2019). The suppression of N_2O fluxes in ECM stands (relative to AM stands) has been reported previously and linked to scavenging of nitrite (Mushinski et al. 2020) by ECM roots and fungi (Holz et al. 2016). Likewise, the availability of inorganic N in the form of NO_3 was highest in AM-associated stands and declined with increasing ECM-associated basal area.

Following nitrification, inorganic N becomes available for gaseous loss as N_2O or N_2 from soil through denitrification. This microbial process accounts for approximately one-third of N outputs from terrestrial ecosystems globally and can contribute to N-limitation (Houlton and Bai 2009). Rates of N_2O-N production declined with increasing ECM-associated basal area, with denitrification rates in AM-associated stands more than five times greater than those in ECM-associated stands on average. These differences indicate reduced losses of N through denitrification in ECM-dominated stands, while showing the potential for reduced retention of N and greater emissions in the forms of N_2O and N_2 in stands dominated by AM-associated trees. It is important to note that these patterns were underlain by significant differences across sites and there remain limited observations of denitrification rates across mycorrhizal gradients; however, these findings are consistent with observations of greater microbial potential for denitrification at sites overlapping with ones in the present study (Mushinski et al. 2020).

Consistent with global patterns of increased C storage per unit N in ECM-dominated systems (Averill et al. 2014), soil C:N increased with ECM-associated basal area in the

gradients explored in this study. This relationship was significant across plots at both sites (Indiana and Massachusetts) but was stronger for plots located in Massachusetts ($p < 0.001$; $R^2 = 0.55$) where soil C:N was higher on average compared to plots located in Indiana ($p < 0.05$; $R^2 = 0.22$) where soil C:N was lower on average. Increased C sequestration relative to N availability in ECM-dominated systems has been linked to slowed decomposition due to competition between free-living heterotrophs and ECM fungi; however, ECM-associated plants may also produce more recalcitrant litter, which could amplify the negative feedback on decomposition (Midgley and Phillips 2014). Our results suggest that greater N fixation rates in AM stands may also explain narrower C:N ratios in these stands.

Although we observed strong structuring of N cycling rates in relation to mycorrhizal abundance, we did not find strong patterns in bacterial N cycling gene abundances. Prior work, including sites overlapping with the present study, indicates that free-living microbial communities in ECM-associated stands are composed of fewer bacteria relative to fungi when compared with communities in AM-associated stands (Cheeke et al. 2017). Similarly, field-exclusion of ECM fungi results in increases in bacterial abundance (Averill and Hawkes 2016). While fungal:bacterial ratios may differ across gradients of mycorrhizal abundance, our findings suggest that the functional profile of the bacterial population can be highly variable. Furthermore, the lack of correlation between functional gene abundances and corresponding flux rates indicates that the limited subset of genes we quantified here are not themselves sufficient for explaining observed patterns in N cycling rates. It is likely that a more complete profile of the microbial community, including the gene abundances of archaea, additional genes within each of N-cycling pathways we explored here, or broader characterization of microbial community composition (e.g., Qin et al. 2019; Kelly et al. 2021) are necessary to more firmly establish links between N-cycling functional groups and fluxes in these forest systems. Additionally, we measured lab potential rates rather than in situ rates, and this limitation may also have contributed to the lack of relationship observed here.

Identifying relationships between gene abundances and ecosystem function has remained a challenge in microbial biogeochemistry (Bier et al. 2015; Rocca et al. 2015; Trivedi et al. 2016). Although commonly assumed otherwise, few forest soil studies find significant gene-function correlations for C and N cycle fluxes (Rocca et al. 2015). Specific relationships are dependent on soil pH, P-availability, and other soil parameters. For example, N_2O flux rates in forest soils were predictable from temperature, dissolved organic carbon, and nitrate availability, but not from the abundance of nitrifiers and denitrifiers in a similar study of gene abundances and flux rates (Qin et al. 2019). However, alternatively, relationships between N-fixation and *nifH* gene abundance have been observed in some studies in temperate forest soils, although these relationships were dependent on P-availability (Tang et al. 2019). Several potential mechanisms have been cited to explain frequent observations of decoupling between flux rates and gene abundances. Gene abundances are thought to better predict process rates than transcript abundances due to the rapid degradation of RNA in the environment; however, gene abundances may also represent dormant and inactive communities. This is a particularly important consideration for processes like N-fixation which are known to be tightly regulated based on abiotic factors, such as resource demand (Reed et al. 2011).

An additional challenge with exploring gene-function relationships involves consideration of the scales at which gene abundances vary compared to flux rates and pool sizes. The abundances of diazotrophs, nitrifiers, and denitrifiers have been shown to vary widely over short timespans and across small distances, while flux rates tend to remain more stable within systems over time (Regan et al. 2017). This limitation also applies to transient pool sizes for ammonium which our analyses may not have captured cohesively. Determining whether frequent observations of nonsignificant relationships between community structure and associated processes are due to a lack of adequate sampling or due to actual biological decoupling will be necessary to fully understand these patterns. Finally, it is important to note that we only characterized a single gene associated with each flux, but there are additional gene targets that could potentially track flux rates more closely, including archaeal contributions to nitrification and other subunits of the nitrous oxide reductase enzyme (Levy-Booth et al. 2014; Erguder et al. 2009). Notably, our focus on bacterial genes excluded ammonium oxidizing archaea, and these groups have been shown to drive differences in nitrification between stand types in the same region (Mushinski et al. 2019).

Overall, we find that mycorrhizal type is associated with major differences in N cycling rates and N availability. Forest stands dominated by ECM-associated fungi show suppressed rates of N-fixation, which may partly explain reduced N stocks relative to C in these systems. We additionally observed suppressed rates of net nitrification and denitrification in the presence of ECM fungi, indicating reduced rates of N losses from these systems. While previous studies have focused on differences in rates of net nitrification across mycorrhizal gradients, the present study suggests that AM-associated stands may have increased rates of inputs from N-fixation as well as exports through denitrification. These findings highlight that mycorrhizal dominance may be a good trait integrator for N cycling in temperate forests, providing an indication of N cycling rates based on dominant mycorrhizal associations (Phillips et al. 2013; Mushinski et al. 2020). We also found that differences in fluxes may

not be underlain by differences in bacterial N cycling gene abundances. As gene abundances are likely to vary across smaller spatial and temporal scales than flux rates, characterizing functional group gene abundances with greater resolution and including additional genes within each pathway may help better elucidate the coupling of structure and flux measurements. Additionally, it will be critical to more fully characterize the full suite of genes and non-bacterial contributions to these fluxes.

Identifying the factors that control microbial N cycling is critical to improving our capacity to quantify inputs and exports of N from temperate forests (Yanai et al. 2012). In the context of global change and anthropogenic sources of nitrogen pollution, shifts in forest community structure will result in changes in N cycling and soil microbial community structure (Averill et al. 2018; Groffman et al. 2018; Jo et al. 2019). This analysis indicates that stand-level mycorrhizal types are associated with significant differences in N cycling activity, including rates of N-fixation, net nitrification, and denitrification, and these are likely to have substantial quantitative impacts on N cycling budgets. Future studies pairing biogeochemical flux measurements with comprehensive microbial community structure data will be necessary to better characterize relationships between community structure and N cycling.

Supplementary Information The online version contains supplementary material available at https://doi.org/10.1007/s00442-021-04966-z.

Acknowledgements Funding was provided by the US National Science Foundation to RPP (DEB, Ecosystem Studies Program; #1153401) and to MS and ACF (DEB, Doctoral Dissertation Improvement Grant, Award # 1701972). Funding was also provided to RPP by the Department of Energy-Office of Biological and Environmental Research-Terrestrial Ecosystem Science Program (Award # DESC0016188). We thank Eddie Brzostek and Mark Sheehan for setting up the gradient plots at the IU Research and Teaching Preserve (RTP) and Michael Chitwood for facilitating research at the RTP properties.

Author contribution statement MS, ACF, JMB, and RPP: conceived and designed the study, MS collected and analyzed the data and wrote the manuscript, with editing by: ACF, JMB, and RPP.

References

Allison SD, Martiny JBH (2008) Resistance, resilience, and redundancy in microbial communities. Proc Natl Acad Sci 105:11512–11519. https://doi.org/10.1073/pnas.0801925105

Arah JRM (1992) New formulae for mass spectrometric analysis of nitrous oxide and dinitrogen emissions. Soil Sci Soc Amer J 56:795–800. https://doi.org/10.2136/sssaj1992.03615995005600030020x

Averill C, Hawkes CV (2016) Ectomycorrhizal fungi slow soil carbon cycling. Ecol Lett 19:937–947. https://doi.org/10.1111/ele.12631

Averill C, Turner BL, Finzi AC (2014) Mycorrhiza-mediated competition between plants and decomposers drives soil carbon storage. Nature 505:543–545. https://doi.org/10.1038/nature12901

Averill C, Dietze MC, Bhatnagar JM (2018) Continental-scale nitrogen pollution is shifting forest mycorrhizal associations and soil carbon stocks. Glob Chang Biol 24:4544–4553. https://doi.org/10.1111/gcb.14368

Averill C, Bhatnagar JM, Dietze MC et al (2019) Global imprint of mycorrhizal fungi on whole-plant nutrient economies. PNAS 116(46):23163–23168

Berthrong ST, Yeager CM, Gallegos-Graves L et al (2014) Nitrogen fertilization has a stronger effect on soil nitrogen-fixing bacterial communities than elevated atmospheric CO_2. Appl Environ Microbiol 80:3103–3112. https://doi.org/10.1128/AEM.04034-13

Bier RL, Bernhardt ES, Boot CM et al (2015) Linking microbial community structure and microbial processes: an empirical and conceptual overview. FEMS Microbiol Ecol 91:fiv113. https://doi.org/10.1093/femsec/fiv113

Bormann BT (1993) Rapid N_2 fixation in pines, alder, and locust: evidence from the sandbox ecosystem study. Ecology 74:583–598. https://doi.org/10.2307/1939318

Bormann BT, Keller CK, Wang D, Bormann FH (2002) Lessons from the sandbox: is unexplained nitrogen real? Ecosystems 5:0727–0733. https://doi.org/10.1007/s10021-002-0189-2

Cheeke TE, Phillips RP, Brzostek ER et al (2017) Dominant mycorrhizal association of trees alters carbon and nutrient cycling by selecting for microbial groups with distinct enzyme function. New Phytol 214:432–442. https://doi.org/10.1111/nph.14343

Chen W, Koide RT, Adams TS et al (2016) Root morphology and mycorrhizal symbioses together shape nutrient foraging strategies of temperate trees. PNAS 113(31):8741–8746

Cornelissen J, Aerts R, Cerabolini B et al (2001) Carbon cycling traits of plant species are linked with mycorrhizal strategy. Oecologia 129:611–619. https://doi.org/10.5301/jn.5000094

Craig ME, Turner BL, Liang C et al (2018a) Tree mycorrhizal type predicts within-site variability in the storage and distribution of soil organic matter. Glob Chang Biol 24:3317–3330. https://doi.org/10.1111/gcb.14132

Craig ME, Lovko N, Flory SL et al (2018b) Impacts of an invasive grass on soil organic matter pools very across a tree-mycorrhizal gradient. Biogeochem. https://doi.org/10.1007/s10533-019-00577-2

Doane TA, Horwáth WR (2003) Spectrophotometric determination of nitrate with a single reagent. Anal Lett 36:2713–2722. https://doi.org/10.1081/AL-120024647

Enanga EM, Casson NJ, Fairweather TA, Creed IF (2017) Nitrous oxide and dinitrogen: the missing flux in nitrogen budgets of forested catchments? Environ Sci Technol 51:6036–6043. https://doi.org/10.1021/acs.est.6b03728

Erguder TH, Boon N, Wittebolle L et al (2009) Environmental factors shaping the ecological niches of ammonia-oxidizing archaea. FEMS Microbiol Rev 33:855–869. https://doi.org/10.1111/j.1574-6976.2009.00179.x

Finzi AC, Berthrong ST (2005) The uptake of amino acids by microbes and trees in three cold-temperate forests. Ecology 86:3345–3353. https://doi.org/10.1890/04-1460

Finzi AC, Van Breemen N, Canham CD (1998) Canopy tree-soil interactions within temperate forests: species effects on soil carbon and nitrogen. Ecol Appl 8:440–446. https://doi.org/10.1890/1051-0761(1998)008[0440:CTSIWT]2.0.CO;2

Finzi AC, Abramoff RZ, Spiller KS et al (2015) Rhizosphere processes are quantitatively important components of terrestrial carbon and nutrient cycles. Glob Chang Biol 21:2082–2094

Gadgil RL, Gadgil PD (1975) Suppression of litter decomposition by mycorrhizal roots of Pinus radiata. N Z J for Sci 5:33–41

Gallet-Budynek A, Brzostek E, Rodgers VL et al (2009) Intact amino acid uptake by northern hardwood and conifer trees. Oecologia 160:129–138. https://doi.org/10.1007/s00442-009-1284-2

Goodale CL (2016) Multiyear fate of a 15N tracer in a mixed deciduous forest: retention, redistribution, and differences by mycorrhizal association. Glob Chang Biol 23(2):867–880. https://doi.org/10.1111/gcb.13483

Groffman PM, Driscoll CT, Duran J et al (2018) Nitrogen oligotrophication in northern hardwood forests. Biogeochem 141(3):523–539

Holz M, Aurangojeb M, Kasimer A et al (2016) Gross nitrogen dynamics in the mycorrhizosphere of an organic forest soil. Ecosystems 19:284–295

Houlton BZ, Bai E (2009) Imprint of denitrifying bacteria on the global terrestrial biosphere. Proc Natl Acad Sci 106:21713–21716. https://doi.org/10.1073/pnas.0912111106

Hsu SF, Buckley DH (2009) Evidence for the functional significance of diazotroph community structure in soil. ISME J 3:124–136. https://doi.org/10.1038/ismej.2008.82

Jo I, Fei S, Oswalt CM, Domke GM, Phillips RP (2019) Shifts in dominant tree mycorrhizal associations in response to anthropogenic impacts. Sci Adv 5:6358

Johnson DJ, Clay K, Phillips RP (2018) Mycorrhizal associations and the spatial structure of an old-growth forest community. Oecologia 186:195–204

Keller AB, Phillips RP (2019a) Leaf litter decay rates differ between mycorrhizal groups in temperate, but not tropical, forests. New Phytol 222:556–564. https://doi.org/10.1111/nph.15524

Keller AB, Phillips RP (2019b) Relationship between belowground carbon allocation and nitrogen uptake in saplings varies by plant mycorrhizal type. Front for Glob Chang 2:81. https://doi.org/10.3389/ffgc.2019.00081

Keller AB, Brzostek ER, Craig ME et al (2021) Root-derived inputs are major contributors to soil carbon in temperate forests, but vary by mycorrhizal type. Ecol Lett 24:626–635. https://doi.org/10.1111/ele.13651

Kelly CN, Schwaner GW, Cumming JR, Driscoll TP (2021) Metagenomic reconstruction of nitrogen and carbon cycling pathways in forest soil: influence of different hardwood tree species. Soil Biol Biochem 156:108226

LeBauer DS, Treseder KK (2008) Nitrogen limitation of net primary productivity in terrestrial ecosystems is globally distributed. Ecology 89:371–379. https://doi.org/10.1890/06-2057.1

Lennon EFE, Houlton BZ (2017) Coupled molecular and isotopic evidence for denitrifier controls over terrestrial nitrogen availability. ISME J 11:727–740. https://doi.org/10.1038/ismej.2016.147

Levy-Booth DJ, Prescott CE, Grayston SJ (2014) Microbial functional genes involved in nitrogen fixation, nitrification and denitrification in forest ecosystems. Soil Biol Biochem 75:11–25. https://doi.org/10.1016/j.soilbio.2014.03.021

Liese R, Lubbe T, Albers NW, Meier IC (2018) The mycorrhizal type governs root exudation and nitrogen uptake of temperate tree species. Tree Physiol 38(1):83–95. https://doi.org/10.1093/treephys/tpx131

Lin G, McCormack ML, Ma C, Guo D (2017) Similar belowground carbon cycling dynamics but contrasting modes of nitrogen cycling between arbuscular mycorrhizal and ectomycorrhizal forests. New Phyt 213:1440–1451

Lin G, Craig MA, Wang X, Zeng D, Jo I, Phillips RP (in revision) Mycorrhizal type influences soil nitrogen dynamics via effects on soil acid-base chemistry. Glob Ecol Biogeo

Lovett GM, Weathers KC, Sobczak WV (2000) Nitrogen saturation and retention in forested watersheds of the Catskill Mountains, New York. Ecol Appl 10:73–84

Lovett GM, Weathers KC, Arthur MA, Schultz JC (2004) Nitrogen cycling in a northern hardwood forest: do species matter? Biogeochem 67:289–308. https://doi.org/10.1023/B:BIOG.0000015786.65466.f5

Lüdecke D, Makowski D, Ben-Shachar MS et al (2020) Assessment of regression models performance. CRAN. https://doi.org/10.5281/zenodo.3952174

McGuire KL, Treseder KK (2010) Microbial communities and their relevance for ecosystem models: decomposition as a case study. Soil Biol Biochem 42:529–535. https://doi.org/10.1016/j.soilbio.2009.11.016

Midgley MG, Phillips RP (2014) Mycorrhizal associations of dominant trees influence nitrate leaching responses to N deposition. Biogeochem 117:241–253. https://doi.org/10.1007/s10533-013-9931-4

Midgley MG, Phillips RP (2016) Resource stoichiometry and the biogeochemical consequences of nitrogen deposition in a mixed deciduous forest. Ecology 97:3369–3378

Montoya JP, Voss M, Kahler P, Capone DG (1996) A simple high-precision, high-sensitivity tracer assay for N2 fixation. Appl Environ Microb 62:986–993

Mushinski RM, Phillips RP, Payne ZC et al (2019) Microbial mechanisms and ecosystem flux estimation for aerobic NOy emissions from deciduous forest soils. Proc Natl Acad Sci 116:2138–2145

Mushinski RM, Payne ZC, Raff JD et al (2020) Nitrogen cycling microbiomes are structured by plant mycorrhizal associations with consequences for nitrogen oxide fluxes in forests. Glob Change Biol 27:1068–1082. https://doi.org/10.1111/gcb.15439

Norman JS, Friesen ML (2017) Complex N acquisition by soil diazotrophs: how the ability to release exoenzymes affects N fixation by terrestrial free-living diazotrophs. ISME J 11:315–326. https://doi.org/10.1038/ismej.2016.127

Phillips RP, Fahey TJ (2006) Tree species and mycorrhizal associations influence the magnitude of rhizosphere effects. Ecology 87:1302–1313

Phillips RP, Brzostek E, Midgley MG (2013) The mycorrhizal-associated nutrient economy: a new framework for predicting carbon-nutrient couplings in temperate forests. New Phytol 199:41–51. https://doi.org/10.1111/nph.12221

Qin H, Xing X, Hou H et al (2019) Linking soil N2O emissions with soil microbial community abundance and structure related to nitrogen cycle in two acid forest soils. Plant Soil 435:95–109. https://doi.org/10.1007/s11104-018-3863-7

R Core Team (2017) R: A language and environment for statistical computing. Vienna, Autria: R Foundation for Statistical Computing

Read DJ, Perez-Moreno J (2003) Mycorrhizas and nutrient cycling in ecosystems-A journey towards relevance? New Phytol 157:475–492. https://doi.org/10.1046/j.1469-8137.2003.00704.x

Reed SC, Townsend AR, Cleveland CC, Nemergut DR (2010) Microbial community shifts influence patterns in tropical forest nitrogen fixation. Oecologia 164:521–531. https://doi.org/10.1007/s00442-010-1649-6

Reed SC, Cleveland CC, Townsend AR (2011) Functional ecology of free-living nitrogen fixation: a contemporary perspective. Annu Rev of Ecol Evol Syst 42:489–512. https://doi.org/10.1146/annurev-ecolsys-102710-145034

Regan K, Stempfhuber B, Schloter M et al (2017) Spatial and temporal dynamics of nitrogen fixing, nitrifying and denitrifying microbes in an unfertilized grassland soil. Soil Biol Biochem 109:214–226. https://doi.org/10.1016/j.soilbio.2016.11.011

Ribbons RR, Kepfer-Rojas S, Kosawang C et al (2018) Context-dependent tree species effects on soil nitrogen transformations and related microbial functional genes. Biogeochem 140:145–160

Rocca JD, Hall EK, Lennon JT et al (2015) Relationships between protein-encoding gene abundance and corresponding process are commonly assumed yet rarely observed. ISME J 9:1693–1699. https://doi.org/10.1038/ismej.2014.252

Shelton AL, Henning JA, Schultz P, Clay P (2014) Effects of abundant white-tailed deer on vegetation animals mycorrhizal fungi and soils. For Ecol Manage 320:39–49. https://doi.org/10.1016/j.foreco.2014.02.026

Sims GK, Ellsworth TR, Mulvaney RL (1995) Microscale determination of inorganic nitrogen in water and soil extracts. Commun Soil Sci Plant Anal 26:303–316. https://doi.org/10.1080/00103629509369298

Sterkenburg E, Clemmensen KE, Ekblad A et al (2018) Contrasting effects of ectomycorrhizal fungi on early and late stage decomposition in a boreal forest. ISME J 12:2187–2197. https://doi.org/10.1038/s41396-018-0181-2

Tang Y, Yu G, Zhang X et al (2019) Different strategies for regulating free-living N2 fixation in nutrient amended subtropical and temperate forest soils. Appl Soil Ecol 136:21–29

Templer PH, Lovett GM, Weathers KC et al (2005) Influence of tree species on forest nitrogen retention in the Catskill Mountains, New York, USA. Ecosystems 8:1–16. https://doi.org/10.1007/s10021-004-0230-8

Trivedi P, Delgado-Baquerizo M, Trivedi C et al (2016) Microbial regulation of the soil carbon cycle: evidence from gene–enzyme relationships. ISME J 10:2593. https://doi.org/10.1038/ismej.2016.65

Venables WN, Ripley BD (2002) Modern applied statistics with S. Springer. Issues of accuracy and scale. Technometrics 45:111. https://doi.org/10.1198/tech.2003.s33

Vitousek PM, Howarth RW (1991) Nitrogen limitation on land and in the sea: How can it occur? Biogeochemistry 13:87–115. https://doi.org/10.1007/BF00002772

Wallenstein MD, Vilgalys RJ (2005) Quantitative analyses of nitrogen cycling genes in soils. Pedobiologia 49:665–672. https://doi.org/10.1016/j.pedobi.2005.05.005

Wurzburger N, Brookshire ENJ (2017) Experimental evidence that mycorrhizal nitrogen strategies affect soil carbon. Ecology 98:1491–1497

Xia J, Wan S (2008) Global response patterns of terrestrial plant species to nitrogen addition. New Phytol 179:428–439. https://doi.org/10.1111/j.1469-8137.2008.02488.x

Yanai RD, Levine CR, Green MB, Campbell JL (2012) Quantifying uncertainty in forest nutrient budgets. J for 110:448–456. https://doi.org/10.5849/jof.11-087

Yanai RD, Vadeboncoeur MA, Hamburg SP et al (2013) From missing source to missing sink: long-term changes in the nitrogen budget of a northern hardwood forest. Environ Sci Technol 47:11440–11448. https://doi.org/10.1021/es4025723